2004

Characterization of LiMxFe1−xPO4 (M = Mg, Zr, Ti) Cathode Materials Prepared by the Sol-Gel Method

G. X. Wang
University of Wollongong, gwang@uow.edu.au

S. Bewlay
University of Wollongong

J. Yao
University of Wollongong, jyao@uow.edu.au

J. H. Ahn
University of Wollongong

S. X. Dou
University of Wollongong, shi@uow.edu.au

See next page for additional authors

Electrochemical and Solid-State Letters, **7** (12) A503-A506 (2004)
1099-0062/2004/7(12)/A503/4/$7.00 © The Electrochemical Society, Inc.

Characterization of $LiM_xFe_{1-x}PO_4$ (M=Mg, Zr, Ti) Cathode Materials Prepared by the Sol-Gel Method

G. X. Wang,*,z Steve Bewlay, Jane Yao, J. H. Ahn, S. X. Dou, and H. K. Liu*

Institute for Superconducting and Electronic Materials, University of Wollongong, New South Wales 2522, Australia

A series of $LiM_xFe_{1-x}PO_4$ (M = Mg,Zr,Ti) phosphates were synthesized via a sol-gel method. Transmission electron microscopy observations show that $LiM_xFe_{1-x}PO_4$ particles consist of nanosize crystals, ranging from 40 to 150 nm. High-resolution TEM analysis reveals that a layer of amorphous carbon was coated on the surface of the $LiM_xFe_{1-x}PO_4$ particles, which substantially increases the electronic conductivity of $LiM_xFe_{1-x}PO_4$ electrodes. The doped $LiM_xFe_{1-x}PO_4$ powders are phase pure. Near full capacity (170 mAh/g) was achieved at the C/8 rate at room temperature for $LiM_xFe_{1-x}PO_4$ electrodes. The doped $LiM_xFe_{1-x}PO_4$ electrodes demonstrated better electrochemical performance than that of undoped $LiFePO_4$ at high rate.
 [DOI: 10.1149/1.1819867]

Manuscript received July 20, 2004. Available electronically November 1, 2004.

Lithium-ion batteries are widely used as advanced power sources for portable electronics, based on the chemistry of $LiCoO_2$ cathode and carbon anode. Because lithium-ion batteries have a much higher energy density than that of lead-acid, Ni-Cd, and Ni-MH batteries, large-scale lithium-ion batteries have great potential for use in future electric vehicles and dispersed energy storage systems. The cost, environmental friendliness, and safety of the electrode materials have become influential considerations in efforts to realize widespread applications of large-size lithium-ion batteries. Recently, lithium iron phosphates have emerged as a new class of cathode materials for lithium-ion batteries because of their low cost, natural abundance, and the nontoxicity of iron.

$LiFePO_4$ has an ordered olivine-type structure (space group *pmnb*), in which Li, Fe, and P atoms occupy octahedral 4a, octahedral 4c, and tetrahedral 4c sites.[1] The Fermi energy of the Fe^{3+}/Fe^{2+} redox couple can be tuned to a useful level by PO_4 polyanions due to polarization of the electrons of the O^{2-} ions toward the P cation within the polyanions.[2-4] However, the separation of the FeO_6 octahedra by PO_4 polyanions in $LiFePO_4$ triphylite significantly reduces the lattice electronic conductivity. This causes poor rate capacity and low utilization of Li in the host structure when it is used as an electrode material in Li-ion cells. Over the past few years, tremendous efforts have been devoted to improving the rate capacity and electrochemical properties of $LiFePO_4$ compounds through different synthesis and characterization techniques.[5-8] Nanosize $LiFePO_4$ powders have been synthesized by heating amorphous $LiFePO_4$ and by using partially oxidized carbon particles as a nucleating agent.[9,10] These nanosize $LiFePO_4$ materials have achieved 90% theoretical capacity at a moderate current rate. The electrochemical conductivity of $LiFePO_4$ can be improved by dispersing copper/silver powders[11] or high surface area carbon black,[12] coating with carbon,[13,14] and doping with alien ions.[15] The overall electrochemical properties can be improved to some extent by the above approaches.

In this paper, we describe synthesizing $LiFePO_4$ and doped $LiM_xFe_{1-x}PO_4$ (M = Mg,Zr,Ti) cathode materials by the sol-gel method. The electrochemical performance of $LiM_xFe_{1-x}PO_4$ (M = Mg,Zr,Ti) cathode materials was found to be enhanced by controlling the crystallinity of the lithium iron phosphates, by carbon coating during the sol-gel synthesis process and by the doping effect.

Experimental

$LiFePO_4$ and doped $LiM_xFe_{1-x}PO_4$ (M = Mg,Zr,Ti) were prepared by the sol-gel process. $Li(OH)\cdot H_2O$ (99.9%, Aldrich), $FeC_2O_4\cdot 2H_2O$ (99%, Aldrich), $NH_4\cdot H_2PO_4$ (97%, Aldrich), $Mg(CH_3CO_2)_2\cdot 4H_2O$ (99%, Aldrich), $Zr(OC_2H_5)_4$ (99%, Aldrich), and $Ti(OCH_3)_4$ (99%, Aldrich) were used as raw chemicals. The stoichiometric reactants were dissolved in deionized water, in which polyacrylic acid and citric acid were added as complexing agents to form a gel. The solution was heated to 85°C under vigorous stirring. The as-formed gel was heat treated at 500°C to decompose the organic compounds under flowing argon gas. The final powders were obtained by sintering the decomposed precursors at 750°C under a flowing gas mixture (5% hydrogen in argon). We employed a slightly reducing atmosphere during the sintering process to prevent the oxidation of Fe^{2+}. Four lithium iron phosphate samples were synthesized with compositions of $LiFePO_4$, $LiMg_{0.01}Fe_{0.99}PO_4$, $LiZr_{0.01}Fe_{0.99}PO_4$, and $LiTi_{0.01}Fe_{0.99}PO_4$. X-ray diffraction (XRD) was performed on the prepared lithium iron phosphates to determine the phase purity using Cu Kα radiation (MO3xHF22, MacScience, Japan). The morphology of $LiM_xFe_{1-x}PO_4$ (M = Mg,Zr,Ti) powders was studied using a high-resolution transmission electron microscope (HRTEM) (300 kV JEOL JEM-3000F with field emission).

The electrochemical evaluation of the synthesized lithium iron phosphates was accomplished by assembling CR2032 coin cells. The electrodes were made by dispersing 84 wt % active materials, 8 wt % carbon black, and 8 wt % polyvinylidene fluoride (PVDF) binder in *n*-methylpyrrolidone (NMP) solvent to form a homogeneous slurry. The slurry was then spread on an Al foil. The coated electrodes were dried in a vacuum oven under a vacuum pressure of 30 Torr at 120°C for 12 h. The electrodes were then pressed at a pressure of 1200 kg/cm^2 to enhance the contact between the active materials and the conductive carbons. The active material loading was about 1.5-2 mg for individual electrode. The cells were assembled in an argon filled glove-box (Mbraun, Unilab, Germany) using lithium metal foil as the counter electrode. The electrolyte was 1 M $LiPF_6$ in a mixture of ethylene carbonate (EC) and dimethyl carbonate (DMC) (1:1 by volume, provided by Merck KgaA, Germany). The cells were galvanostatically charged and discharged over a voltage range of 2.75-4.3 V at different rates. Cyclic voltammetry (CV) measurements were performed using an EG&G scanning potentiostat (model 362) at a scanning rate of 0.1 mV/s.

Results and Discussion

XRD patterns of $LiFePO_4$ and doped $LiM_xFe_{1-x}PO_4$ (M = Mg,Ti, and Zr) are shown in Fig. 1. All diffraction lines are indexed to an orthorhombic crystal structure (space group *pmnb*, triphylite). No phase impurities were detected by XRD. We intended to substitute the dopant ions Mg^{2+}, Ti^{4+}, and Zr^{4+} for Fe^{2+} on the M2 sites in the olivine structure. A previous report found the detectable impurity Li_3PO_4 in doped $LiM_xFe_{1-x}PO_4$ prepared by solid-

* Electrochemical Society Active Member.
z E-mail: gwang@uow.edu.au

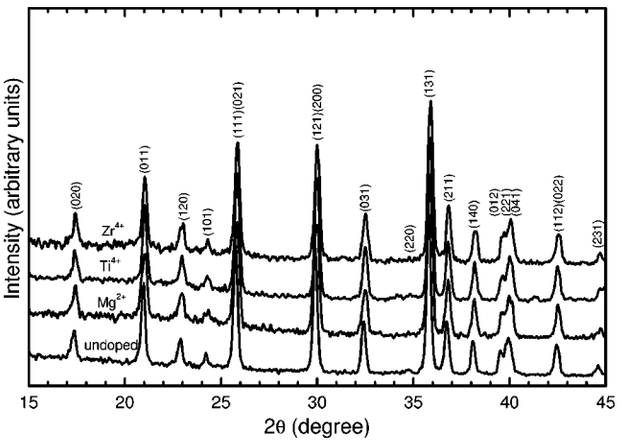

Figure 1. XRD patterns of lithium iron phosphates.

state reaction, even at a very low dopant level.[15] In contrast, detectable precipitation of Li_3PO_4 impurity was not found in the synthesized $LiM_{0.01}Fe_{0.99}PO_4$ (M = Mg,Ti, and Zr) compounds, indicating that the sol-gel process can produce purer solid-state solutions than the solid-state reaction process. During the synthesis process, the reactants were mixed homogeneously in solution and then formed gel complexes. Therefore, a homogeneous distribution of composition elements is expected. The elemental mapping was performed on a $LiFePO_4$ grain by HRTEM facility. Figure 2a and b shows the respective elemental mappings of Fe and P in $LiFePO_4$ compounds. A uniform distribution of Fe and P was observed in microdomain.

A TEM image of the $LiFePO_4$ powders is shown in Fig. 3a. The powders have a primary crystal size ranging from 40 to 150 nm, and the crystals form loose agglomerates. The small crystallinity and porous agglomerate structure allow easy penetration of the electrolyte and provide a short pathway for lithium diffusion in the active material crystals. To examine the fine structure of the synthesized lithium iron phosphates, HRTEM was performed on the powder samples. Figure 3b shows a HRTEM image of a $LiFePO_4$ crystal

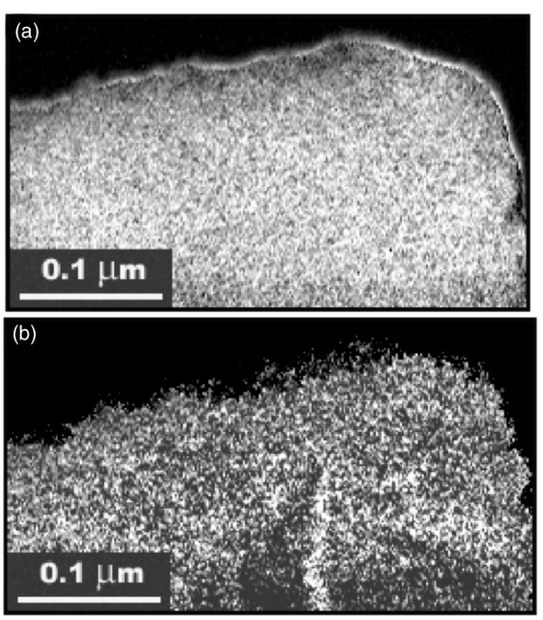

Figure 2. EDS element mapping of (a) Fe (b) P in $LiFePO_4$ compound.

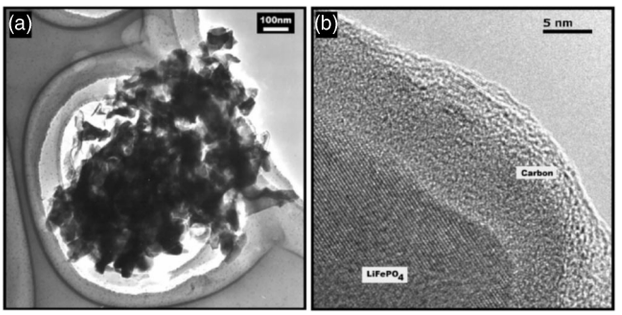

Figure 3. (a) TEM image of $LiFePO_4$ powders. (b) HRTEM image of single $LiFePO_4$ crystal.

edge. Spot EDX analysis confirmed that the outside layers are amorphous carbon and the inside crystallites are lithium iron phosphates. It clearly demonstrated that a thin layer of unorganized carbon was coated on the surface of the $LiFePO_4$ crystals. During the synthesis process, the gel complexes and precursors were sintered in an inert atmosphere. Carbon was formed from the decomposition of the organic compounds. The carbon content was determined by thermogravimetric (TG) and chemical analysis. The lithium iron phosphates prepared by the sol-gel process contain ~7.5 wt % carbon. Because the individual lithium iron phosphate crystals are wired together by the coated carbon layer, it was expected that the carbon coating on the lithium iron phosphate crystals would dramatically increase the electronic conductivity of the electrodes. We pressed the doped and undoped lithium iron phosphates into disk-shaped pellets. The electronic conductivities were measured by the two-point dc method. All pellets exhibited a high electronic conductivity of $\sim 10^{-1}$ S/cm at room temperature. Such a high electronic conductivity mainly comes from the carbon coating. The electronic conductivity of the compressed pellets is dominated by the carbon network. Therefore, the contribution of the doping effect to the enhancement of the electronic conductivity on the level of the bulk materials cannot be distinguished by dc measurement. However, as indicated in Ref. 15, the doping element induces p-type semiconductivity and might increase the electronic conductivity of the materials on the lattice level, which would be beneficial for the electrochemical properties.

Typical cyclic voltammograms (CVs) of $LiFePO_4$ and doped $LiM_xFe_{1-x}PO_4$ (M = Mg,Ti, and Zr) are shown in Fig. 4. The positions of the reduction and oxidation peaks for $LiFePO_4$ and doped $LiM_xFe_{1-x}PO_4$ (M = Mg,Ti, and Zr) are 3.34 and 3.52 V, respectively, *vs.* Li/Li^+. The redox potentials were not influenced by the

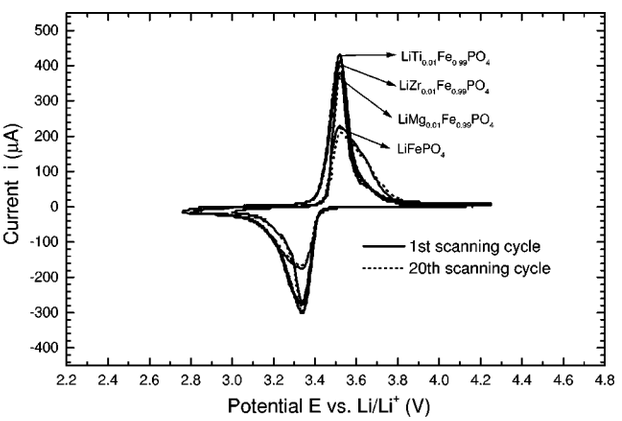

Figure 4. CVs of doped and undoped $LiFePO_4$ electrodes.

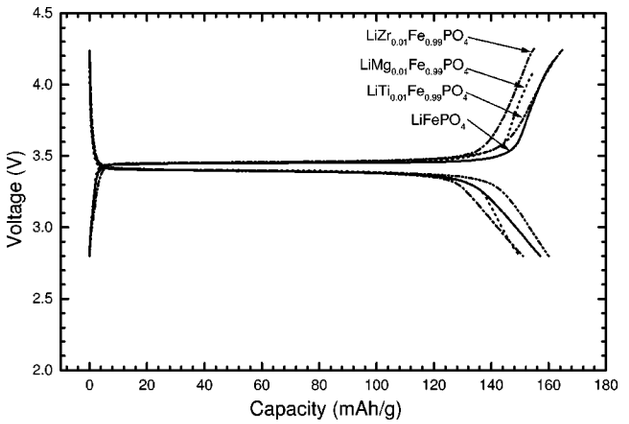

Figure 5. Charge/discharge curve in the first cycle for doped and undoped $LiFePO_4$ electrodes.

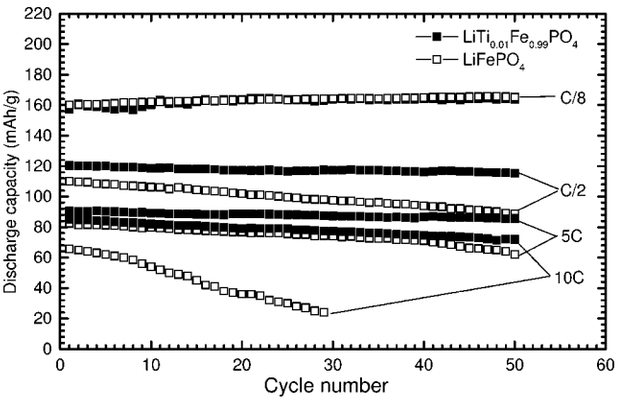

Figure 6. Discharge capacity *vs.* cycle number at different charge/discharge rates for $LiFePO_4$ and $LiTi_{0.01}Fe_{0.99}PO_4$ electrodes.

doping element, indicating the stable nature of the dopant ions Mg^{2+}, Ti^{4+}, and Zr^{4+}. In the doped $LiM_xFe_{1-x}PO_4$ (M = Mg,Ti, and Zr) structure, the Fe^{2+}/Fe^{3+} redox couples are responsible for the gain and loss of electrons that accompany lithium insertion and extraction. It is unlikely that the dopant ions participate in the redox reactions, which is evidenced by the lack of any additional redox peaks in the CV curves. The undoped $LiFePO_4$ electrode has a broad oxidation and reduction peaks in CV curves. In contrast, all three doped $LiFePO_4$ electrodes demonstrated sharp redox peaks in CV curves. This could be related to the difference of intrinsic electronic conductivity of doped and undoped lithium iron phosphates. The doped samples show higher electrochemical reactivity for lithium insertion and extraction reaction at a scanning rate of 0.1 mV/s. The reproducibility of the oxidation and reduction peaks in the CV curves is excellent for all doped and undoped $LiFePO_4$ electrodes.

Figure 5 shows the charge/discharge voltage profiles of $LiFePO_4$ and doped $LiMn_{0.01}Fe_{1.99}PO_4$ (M = Mg, Ti, and Zr) electrodes in the first cycle. The cells were charged and discharged at a rate of C/8. The initial capacities for $LiFePO_4$ and doped $LiMn_{0.01}Fe_{1.99}PO_4$ (M = Mg, Ti, and Zr) electrodes are almost the same, between 150 and 160 mAh/g (approaching the theoretical capacity of 170 mAh/g). From the shape of the charge and discharge profiles, both the doped and undoped lithium iron phosphate electrodes exhibited a flat charge and discharge plateau, indicating little polarization. The small polarization of the lithium iron phosphate electrodes should be ascribed to the high electronic conductivity of the materials. The carbon coating can increase the surface electronic conduction. Furthermore, the element doping can intrinsically enhance the bulk electronic conductivity of $LiFePO_4$ materials by inducing an increased p-type semiconductivity.[15] However, the influence of the doping effect on the electrochemical performance was not shown at low charge/discharge rate, since the carbon coating already dramatically increases the electronic conductivity of the materials. The cyclability of the $LiFePO_4$ and doped $LiTi_{0.01}Fe_{1.99}PO_4$ electrodes at the C/8 rate is shown in Fig. 6. The lithium iron phosphate electrodes show an initial discharge capacity of ~160 mAh/g. Their discharge capacities gradually increase with cycling and reach a maximum of 165 mAh/g after 20 cycles, then become stable. Both the doped and undoped lithium iron phosphate electrodes show good cyclability.

To distinguish the doping effect on the electrochemical performance of lithium iron phosphates, we performed high rate cycling. Figure 6 shows the results for $LiFePO_4$ and doped $LiTi_{0.01}Fe_{1.99}PO_4$ electrodes at different high cycling rates. The doped sample demonstrated better performance than the undoped one at high charge/discharge rate. This effect becomes easily distinguishable at the high charge/discharge rate of 10C. When the electrodes are charged and discharged at high rate, the polarization of the electrodes due to electronic conductivity becomes an influential factor determining the kinetics of the electrochemical reaction of the electrodes. Lithium insertion and extraction in $LiFePO_4$ electrodes is accompanied by electron transfer not only in the particle surface but also inside the crystals. Because the doping effect induces the increased semiconductivity of $LiFePO_4$, which enhances the electronic conductivity of the electrode materials on the crystal level, electron transfer in doped $LiFePO_4$ would be more facilitated than that in undoped $LiFePO_4$. This is because the individual undoped $LiFePO_4$ crystals are still insulator. Therefore, the doped samples demonstrated better overall electrochemical performance at high rate.

Conclusions

Phase-pure $LiM_xFe_{1-x}PO_4$ (M = Mg,Zr,Ti) compounds were prepared by sol-gel synthesis. A layer of carbon was coated on the surface of the lithium crystals, which is known to dramatically enhance the electronic conductivity. The sol-gel synthesis induces nanocrystallinity, which could provide short paths for lithium diffusion. The Ti-doped and undoped lithium iron phosphates demonstrated a stable discharge capacity of approximately 160-165 mAh/g, almost approaching the theoretical capacity, at a low rate of C/8. The good electronic conductivity and nanocrystallinity could contribute to the excellent electrochemical performance of the lithium iron phosphates. We found that the doping effect can significantly enhance the electrochemical performance of lithium iron phosphates at high charge/discharge rates.

Acknowledgment

This work was supported by the Australia Research Council through the ARC Center for Nanostructured Electromaterials and industrial partner Sons of Gwalia Ltd.

The University of Wollongong assisted in meeting the publication costs of this article.

References

1. V. A. Streltsov, E. L. Belokoneva, V. G. Tsirelson, and N. Hansen, *Acta Crystallogr., Sect. B: Struct. Sci.*, **49**, 147 (1993).
2. K. S. Nanjundaswamy, A. K. Padhi, J. B. Goodenough, S. Okada, H. Ohtsuka, H. Arai, and J. Yamaki, *Solid State Ionics*, **92**, 1 (1996).
3. A. K. Padhi, K. S. Nanjundaswamy, and J. B. Goodenough, *J. Electrochem. Soc.*, **144**, 1188 (1997).
4. A. K. Padhi, K. S. Nanjundaswamy, C. Masquelier, S. Okada, and J. B. Goodenough, *J. Electrochem. Soc.*, **144**, 1609 (1997).
5. M. Takahashi, S. Tobishima, K. Takei, and Y. Sakurai, *J. Power Sources*, **97-98**, 508 (2001).
6. J. Barker, M. Y. Saidi, and J. L. Swoyer, *Electrochem. Solid-State Lett.*, **6**, A53 (2003).

7. A. S. Andersson, B. Kalska, L. Häggström, and J. O. Thomas, *Solid State Ionics*, **130**, 41 (2000).
8. A. S. Andersson, J. O. Thomas, B. Kalska, and L. Häggström, *Electrochem. Solid-State Lett.*, **3**, 66 (2000).
9. P. P. Prosini, M. Carewska, S. Scaccia, P. Wisniewski, S. Passerini, and M. Pasquali, *J. Electrochem. Soc.*, **149**, A886 (2002).
10. H. Huang, S.-C. Yin, and L. F. Nazar, *Electrochem. Solid-State Lett.*, **4**, A170 (2001).
11. F. Croce, A. D. Epifanio, J. Hassoun, A. Deptula, T. Olczac, and B. Scrosati, *Electrochem. Solid-State Lett.*, **5**, A47 (2002).
12. P. P. Prosini, D. Zane, and M. Pasquali, *Electrochim. Acta*, **46**, 3517 (2001).
13. S. Franger, F. Le Cras, C. Bourbon, and H. Rouault, *Electrochem. Solid-State Lett.*, **5**, A231 (2002).
14. S. F. Yang, Y. N. Song, P. Y. Zavalij, and M. Stanley Whittingham, *Electrochem. Commun.*, **4**, 239 (2002).
15. S.-Y. Chung, J. Bloking, and Y.-M. Chiang, *Nat. Mater.*, **1**, 123 (2002).